

Many-body superradiance and dynamical symmetry breaking in waveguide QED

Silvia Cardenas-Lopez, Stuart J. Masson, Zoe Zager, and Ana Asenjo-Garcia*

Department of Physics, Columbia University, New York, NY 10027, USA

(Dated: October 7, 2022)

The many-body decay of extended collections of two-level systems remains an open problem. Here, we investigate whether an array of qubits coupled to a one-dimensional bath undergoes Dicke superradiance, a process whereby a completely inverted system synchronizes as it decays, generating correlations between qubits via dissipation. This leads to the release of all the energy in the form of a rapid photon burst. We derive the minimal conditions for the burst to happen as a function of the number of qubits, the chirality of the waveguide, and the single-qubit optical depth, both for ordered and disordered ensembles. Many-body superradiance occurs because the initial fluctuation that triggers the emission is amplified through the decay process. We show that this avalanche-like behavior leads to a dynamical spontaneous symmetry breaking, where most photons are emitted into either the left- or the right-propagating optical modes, giving rise to an emergent chirality. Superradiant bursts may be a smoking gun for the generation of correlated photon states of exotic quantum statistics. This physics can be explored in diverse setups, ranging from atoms close to nanofibers to superconducting qubits coupled to transmission lines.

The decay rate of a single emitter is dictated by its radiative environment [1–3]. This realization contributed to the development of cavity quantum electrodynamics (QED). Here, highly-reflecting mirrors isolate a single optical mode, yielding a localized (or zero-dimensional) reservoir for the emitter, which enhances its decay into the cavity.

The case of a one-dimensional (1D) bath is studied in the field of waveguide QED, where an atom is interfaced with a propagating optical mode. Recent years have seen tremendous progress in waveguide QED experiments, with platforms including cold atoms coupled to optical nanofibers [4–7] and photonic crystal waveguides [8–10], and superconducting qubits coupled to microwave transmission lines [11–13]. Besides altering the decay properties, interfacing several emitters with 1D propagating modes allows one to engineer long-range atom-atom interactions [14–16].

The environment not only modifies the decay properties of a single emitter, but also determines the many-body decay of a multiply-excited ensemble. A paradigmatic example of many-body decay is that of Dicke superradiance: a collection of fully-inverted emitters synchronize as they decay, emitting photons in a short and bright pulse [17, 18]. Despite its many-body nature, this problem is exactly solvable in a cavity due to the imposed symmetry, which restricts the dynamics to a small subset of states of the (otherwise exponentially-large) Hilbert space. In extended systems, where the bath is not zero-dimensional and atom-atom interactions depend on their positions, many-body decay remains an open problem [18–31].

Here, we investigate the decay of a fully inverted array of qubits into a 1D bath. We leverage previous work [29] to bypass the exponential growth of the Hilbert space by studying the early dynamics, and set constraints on the number of qubits needed to observe superradiance.

We investigate chiral and bidirectional waveguides, interfaced with ordered arrays and disordered ensembles. We identify superradiance as a mechanism to spontaneously break mirror symmetry, giving rise to an emergent chirality whereby most photons are emitted in one direction. We confirm this hypothesis by computing the probability distribution of directional emission, finding the likelihood of emitting all photons in one direction is enhanced.

We consider N qubits of resonance frequency ω_0 coupled to a 1D photonic channel, as shown in Fig. 1(a). The guided mode of the waveguide mediates interactions between qubits. Tracing out the photonic degrees of freedom under a Born-Markov approximation, the evolution of the qubits' density matrix $\hat{\rho} = |\psi\rangle\langle\psi|$ in the rotating frame is described by the master equation [32, 33]

$$\dot{\hat{\rho}} = -\frac{i}{\hbar} [\mathcal{H}_L + \mathcal{H}_R, \hat{\rho}] + \mathcal{L}_g[\hat{\rho}] + \mathcal{L}_{ng}[\hat{\rho}]. \quad (1)$$

Here, the Hamiltonians $\mathcal{H}_{\{L,R\}}$ allow for the possibility of distinct coupling to the left- and right-propagating waveguide modes (at rates $\Gamma_{\{L,R\}}$ for a single qubit), and read [34]

$$\mathcal{H}_L = -\frac{i\hbar\Gamma_L}{2} \sum_{i<j} e^{ik_{1D}|z_i-z_j|} \hat{\sigma}_{eg}^i \hat{\sigma}_{ge}^j + \text{H. c.}, \quad (2a)$$

$$\mathcal{H}_R = -\frac{i\hbar\Gamma_R}{2} \sum_{i>j} e^{ik_{1D}|z_i-z_j|} \hat{\sigma}_{eg}^i \hat{\sigma}_{ge}^j + \text{H. c.}, \quad (2b)$$

where $\hat{\sigma}_{ge}^i = |g_i\rangle\langle e_i|$ is the coherence operator between the ground and excited states of qubit i at position z_i , and k_{1D} is the photon wavevector. The total decay rate of a single qubit into the waveguide is denoted as $\Gamma_{1D} = \Gamma_L + \Gamma_R$. The Lindblad operators $\mathcal{L}_g[\hat{\rho}]$ and $\mathcal{L}_{ng}[\hat{\rho}]$ describe decay of the qubits to guided and non-guided modes, respectively, and read

$$\mathcal{L}_\alpha[\hat{\rho}] = \sum_{i,j=1}^N \frac{\Gamma_{ij}^\alpha}{2} (2\hat{\sigma}_{ge}^j \hat{\rho} \hat{\sigma}_{eg}^i - \hat{\rho} \hat{\sigma}_{eg}^i \hat{\sigma}_{ge}^j - \hat{\sigma}_{eg}^i \hat{\sigma}_{ge}^j \hat{\rho}), \quad (3)$$

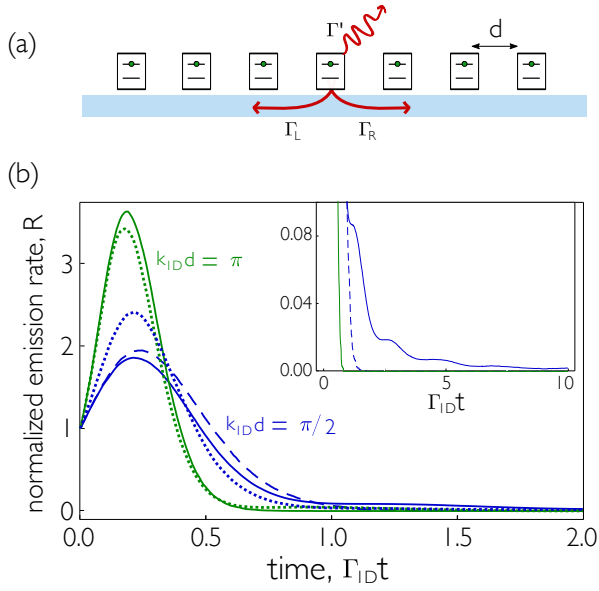


FIG. 1. Many-body superradiance from an ensemble of qubits coupled to a waveguide. (a) Schematic: an array of N qubits of lattice constant d interact via a 1D bath, which supports propagation of photons of wavevector k_{1D} . The single-qubit decay rates into the left and right-propagating modes of the waveguide are Γ_L and Γ_R , respectively, and any other parasitic decay is denoted by Γ' . (b) Rate of photon emission into the waveguide for an array of $N = 16$ qubits coupled to a bidirectional (solid lines) and a chiral (dotted lines) waveguide with $\Gamma_R = 3\Gamma_L$ and $\Gamma' = 0$. Dashed lines show the calculation without Hamiltonian contribution (for the bidirectional waveguide) which is significant at late times (inset).

where $\Gamma_{ij}^g = \Gamma_L e^{ik_{1D}(z_j - z_i)} + \Gamma_R e^{-ik_{1D}(z_j - z_i)}$ and $\Gamma_{ij}^{ng} = \Gamma' \delta_{ij}$. We consider that the latter decay is not collective, either because it represents local parasitic decay or because qubits are far separated and interactions via non-guided modes are negligible.

Emission of photons into the waveguide is correlated, due to the shared bath. This is captured by collective jump operators, found by diagonalizing the $N \times N$ Hermitian matrix \mathbb{F} of elements Γ_{ij}^g [24, 35]. Photons can only be emitted into the left- or right-propagating modes, and thus \mathbb{F} has only two non-zero eigenvalues. The decay into the waveguide is described in terms of two independent decay channels as

$$\mathcal{L}_g[\hat{\rho}] = \sum_{\nu=+,-} \frac{\Gamma_\nu}{2} \left(2\hat{\mathcal{O}}_\nu \hat{\rho} \hat{\mathcal{O}}_\nu^\dagger - \hat{\rho} \hat{\mathcal{O}}_\nu^\dagger \hat{\mathcal{O}}_\nu - \hat{\mathcal{O}}_\nu^\dagger \hat{\mathcal{O}}_\nu \hat{\rho} \right), \quad (4)$$

where $\hat{\mathcal{O}}_\nu$ are collective jump operators and Γ_ν are collective decay rates, found as the eigenvectors and eigenvalues of \mathbb{F} , respectively. The $\{+, -\}$ notation indicates that the action of $\hat{\mathcal{O}}_{+,-}$ generates a photon in a superposition of left- and right-propagating modes.

A fully inverted initial state (i.e., $|\psi(t=0)\rangle = |e\rangle^{\otimes N}$) will decay due to vacuum fluctuations, leading to the emission of photons into the waveguide at a (normalized)

rate

$$R(t) = \frac{1}{N\Gamma_{1D}} \sum_{\nu=+,-} \Gamma_\nu \langle \hat{\mathcal{O}}_\nu^\dagger \hat{\mathcal{O}}_\nu \rangle. \quad (5)$$

For large enough atom numbers and $\Gamma' = 0$, a superradiant burst occurs for any lattice constant, as shown in Fig. 1(b) for ordered arrays. Calculations are performed using quantum trajectories [36, 37] (see Supplemental Information (SI) for details on numerical calculations).

Maximal superradiance occurs in a bidirectional waveguide (i.e., with $\Gamma_R = \Gamma_L$), at the so-called “mirror configuration” (with $k_{1D}d = n\pi$ with $n \in \mathbb{N}$ [38–40]), as this situation corresponds to that studied by Dicke.

Dissipative dynamics are the main driving mechanism for the burst. The coherent interactions (i.e., Hamiltonian) only start contributing significantly beyond the time of maximum emission. At later times, the Hamiltonian plays a very significant role, as shown in the inset. For low excitation densities, the photon emission rate diminishes and the Hamiltonian contributes to the trapping of the excitation in dark states that do not decay [16].

As we postulated in prior work [29], the minimal condition for a burst to occur is that the first photon enhances the emission of the second. This can be expressed as a condition on the second-order correlation function at $t = 0$, which results in constraints on the number of qubits, their separation, and the ratio Γ_{1D}/Γ' . We adapt the calculation from Ref. [27] of “directional superradiance” and define the conditioned second-order correlation function,

$$\tilde{g}^{(2)}(0) = \frac{\sum_{\nu=+,-} \sum_{\mu=+,-,i} \Gamma_\nu \Gamma_\mu \langle \hat{\mathcal{O}}_\mu^\dagger \hat{\mathcal{O}}_\nu^\dagger \hat{\mathcal{O}}_\nu \hat{\mathcal{O}}_\mu \rangle}{\left(\sum_{\nu=+,-} \Gamma_\nu \langle \hat{\mathcal{O}}_\nu^\dagger \hat{\mathcal{O}}_\nu \rangle \right) \left(\sum_{\mu=+,-,i} \Gamma_\mu \langle \hat{\mathcal{O}}_\mu^\dagger \hat{\mathcal{O}}_\mu \rangle \right)}. \quad (6)$$

Here, sums over \pm account for waveguide emission, while sums in i account for local decay. This condition calculates whether there is an enhancement of the photon emission rate into the waveguide only (instead of into all possible decay channels). The minimal condition for superradiant emission of photons into the waveguide is found by imposing $\tilde{g}^{(2)}(0) > 1$. For an ensemble of initially-inverted qubits this condition becomes

$$\text{Var} \left(\frac{\{\Gamma_\nu\}}{\Gamma_{1D}} \right) > 1 + \frac{\Gamma'}{\Gamma_{1D}}, \quad (7)$$

where $\text{Var}(\cdot)$ is the variance (see SI for details). This expression is general, i.e., it applies to systems with any number of qubits, in both disordered or ordered spatial configurations, coupled to waveguides with any degree of chirality. A burst will occur if there are only a few dominant decay channels (thus maximizing the variance),

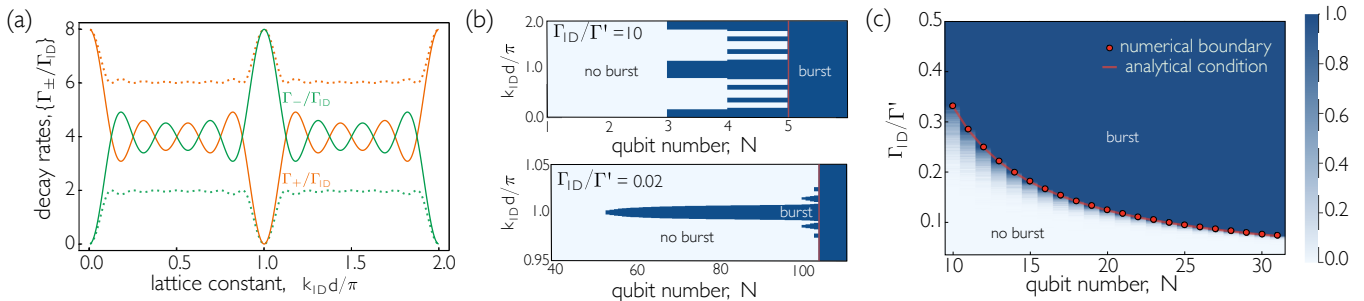


FIG. 2. Predictions of superradiance for ordered and disordered ensembles. (a) Collective decay rates into a bidirectional (solid lines) and a chiral (dotted lines) waveguide for $N = 8$ qubits. The single-qubit decay rates for the chiral waveguide are $\Gamma_R = 0.75\Gamma_{1D}$ and $\Gamma_L = 0.25\Gamma_{1D}$. (b) Crossover between the burst (dark blue) and no-burst (pale blue) regions in ordered arrays coupled to a bidirectional waveguide. (c) Probability of having a burst in a bidirectional waveguide for spatially-disordered ensembles of qubits randomly placed over a section of length $k_{1D}z_{\max} = 200\pi$ (see SI for details). In (b,c) the red line shows the qubit number that guarantees a burst regardless of separation, as given by Eq. (10).

and if collective decay overcomes local loss (represented by the last term of the equation). As emission is constrained to 1D, there are at most two bright channels, while $N - 2$ are dark (i.e., of zero decay rate). Therefore, the conditions for a burst are more easily satisfied than for arrays in free space [25, 29, 30].

For ordered arrays of lattice constant d , the two collective decay rates admit the analytical form

$$\Gamma_{\pm} = \frac{N\Gamma_{1D}}{2} \pm \sqrt{\frac{N^2(\Gamma_L - \Gamma_R)^2}{4} + \Gamma_L\Gamma_R \frac{\sin^2 Nk_{1D}d}{\sin^2 k_{1D}d}}. \quad (8)$$

As shown in Fig. 2(a), the two decay rates are generally distinct and finite, leading to competition between the \pm channels. Nevertheless, in two scenarios there is only a single bright channel. The first scenario is that of a perfectly-chiral waveguide, for which $\Gamma_+ = N\Gamma_{1D}$ and $\Gamma_- = 0$. While there is only one jump operator for any lattice constant, this situation is not exactly that studied by Dicke, due to the non-zero coherent evolution. The second scenario happens at the mirror configuration, for waveguides of arbitrary chirality. For bidirectional waveguides, the coherent interactions mediated by the Hamiltonian vanish and the system reduces to the model originally studied by Dicke.

The scenario of maximal competition between decay channels occurs whenever their rates are identical. This happens only for bidirectional waveguides at “degeneracy points” (with $k_{1D}d = n\pi/N$), where the total length of the array and the guided mode wavelength $\lambda_{1D} = 2\pi/k_{1D}$ are commensurate. Commensurability endows the system with translation symmetry, giving rise to emergent periodic or anti-periodic boundary conditions (see SI). Any level of chirality breaks the translation symmetry and opens a gap in the decay spectrum.

For ordered arrays, the minimal burst condition reads

$$\frac{N(\Gamma_L^2 + \Gamma_R^2)}{\Gamma_{1D}^2} + 2\frac{\Gamma_L\Gamma_R}{N\Gamma_{1D}^2} \frac{\sin^2 Nk_{1D}d}{\sin^2 k_{1D}d} > 2 + \frac{\Gamma'}{\Gamma_{1D}}. \quad (9)$$

The condition reduces to $(N - 2)\Gamma_{1D} > \Gamma'$ if the qubits are either in the mirror configuration or coupled to a perfectly-chiral waveguide.

A few qubits can produce a superradiant burst if $\Gamma_{1D} \gg \Gamma'$, such as for superconducting qubit experiments. However, where there is larger independent emission, such as in nanofibers, dephasing in the array quenches the superradiant burst. Nevertheless, as shown in Fig. 2(b), this effect can always be overcome by increasing the number of qubits, and a burst arises regardless of the spatial configuration, provided that N is large enough. For an array of $N \gg 1$ qubits coupled to a bidirectional waveguide not in the mirror configuration, the sinusoidal term does not scale with N and can be ignored. This yields the condition $(N - 4)\Gamma_{1D} > 2\Gamma'$. A superradiant burst at $k_{1D}d = n\pi$ is achievable with half of the qubits needed for most other spatial configurations.

For disordered systems we obtain the minimal burst condition in terms of single-qubit decay rates by placing a lower bound on the trace of Γ^2 , as the eigenvalues do not admit an analytical form. As shown in the SI, $\text{Tr}[\Gamma^2] \geq N^2(\Gamma_R^2 + \Gamma_L^2)$, and the burst is guaranteed to happen for

$$N\frac{\Gamma_L^2 + \Gamma_R^2}{\Gamma_{1D}^2} > 2 + \frac{\Gamma'}{\Gamma_{1D}}. \quad (10)$$

As shown in Fig 2(c), disordered systems saturate this bound, while ordered systems may display a burst for lower N due to interference effects [as shown by Eq. (9) and Fig 2(b)].

Generically, correlations imparted by the jump operators not only produce an accelerated emission of the second photon, but also of the subsequent ones. This “avalanche”-like nature of photon emission implies that an initial fluctuation is amplified throughout the decay process. For instance, if the first photon is measured by a detector at the right of the array, it is then very likely that the subsequent ones are also detected in that direction. This process gives rise to an emergent chirality even

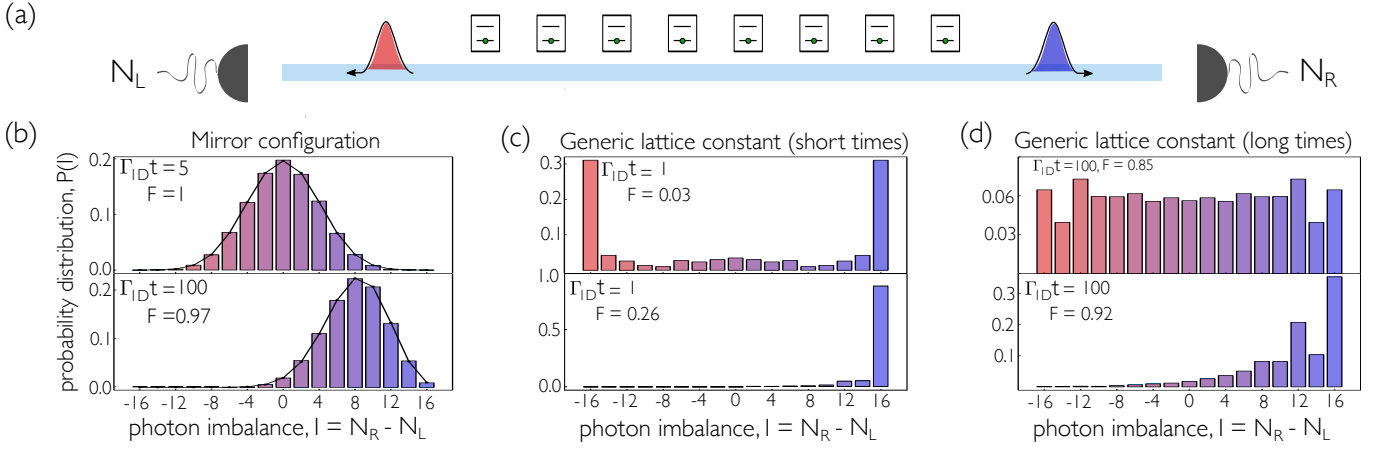


FIG. 3. Emergence of chirality via many-body decay. (a) Superradiant decay leads to successive photon emission, whose directionality can be investigated by detectors placed at both sides of the waveguide and computing the statistics of the imbalance between the number of right- and left-propagating photons. (b)-(d) Directional photon imbalance for an array of 16 qubits emitting into a symmetric (top) and asymmetric (bottom) waveguide, with $\Gamma' = 0$. For the latter, $\Gamma_R = 3\Gamma_L$. The lattice constant is (b) $k_{1D}d = \pi$ and (c,d) $k_{1D}d = \pi/\sqrt{3}$. In (c,d), we investigate short and long times respectively. In each case, only trajectories that reach $|g\rangle^{\otimes N}$ before time t are accounted for, with F denoting the fraction of finished trajectories.

in the case of a bidirectional waveguide. To explore this physics, we unravel $\mathcal{L}_g[\rho]$ in terms of a different pair of operators,

$$\hat{\mathcal{G}}_{L/R} = \frac{1}{\sqrt{N}} \sum_{i=1}^N e^{\pm i k_{1D} d i} \hat{\sigma}_{ge}^i, \quad (11)$$

which describe the emission of photons to the left- and right-propagating modes with rates $\Gamma_{L/R}$.

The measurement of the first photon at either the left or right detectors is a stochastic process due to the uncorrelated initial state. The probability of emitting the first photon in each direction depends only on the relative decay rate of each operator, i.e., $p_{L(R)} = \Gamma_{L(R)}/\Gamma_{1D}$. Assuming that the first photon is emitted to the left, we analyze how this emission affects the subsequent one by splitting the correlation function of Eq. (6) into its directional components, i.e.,

$$\tilde{g}^{(2)}(0) = \frac{2\Gamma_L\Gamma_R}{\Gamma_{1D}^2} \tilde{g}_{LR}^{(2)}(0) + \frac{\Gamma_R^2 + \Gamma_L^2}{\Gamma_{1D}^2} \tilde{g}_{LL}^{(2)}(0), \quad (12)$$

where $\tilde{g}_{\alpha\beta}^{(2)}(0) = \langle \hat{\sigma}_\alpha^\dagger \hat{\sigma}_\beta^\dagger \hat{\sigma}_\beta \hat{\sigma}_\alpha \rangle / (\langle \hat{\sigma}_\alpha^\dagger \hat{\sigma}_\alpha \rangle \langle \hat{\sigma}_\beta^\dagger \hat{\sigma}_\beta \rangle)$, and we have assumed that all the photons are emitted into the waveguide (i.e., $\Gamma' = 0$).

The emergent chirality is evident at the level of just two photons. The correlation functions of Eq. (12) read

$$\tilde{g}_{LL}^{(2)}(0) = 2 - \frac{2}{N}, \quad (13a)$$

$$\tilde{g}_{LR}^{(2)}(0) = 1 - \frac{2}{N} + \frac{1}{N^2} \frac{\sin^2 N k_{1D} d}{\sin^2 k_{1D} d}. \quad (13b)$$

For large N , the second photon is twice as likely to follow the direction of the first. The mirror configuration is an exception, as $\hat{\mathcal{G}}_{L/R}$ are identical.

For a bidirectional waveguide, this emergent chirality is akin to a process of spontaneous symmetry breaking, where the mirror symmetry is broken dynamically. A large superradiant burst implies that, for a single realization, most photons are emitted in one direction. Of course, the symmetry is recovered when averaged over realizations, as the first photon is randomly emitted into either direction.

We characterize this behavior by counting the photons emitted in both directions and computing the “photon imbalance”, as shown in Fig. 3(a). For a single quantum trajectory – in which the atoms evolve from $|e\rangle^{\otimes N}$ to $|g\rangle^{\otimes N}$ via both coherent evolution with a non-Hermitian Hamiltonian and decay by the action of the jump operators – we define the photon imbalance as the difference in the number of times that the two jump operators act. This corresponds to counting the final number of photons emitted to the right (N_R) and left (N_L) with imbalance

$$I = N_R - N_L. \quad (14)$$

I must be $\{-N, -N+2, \dots, N\}$, as the number of emitted photons is fixed (i.e., $N_R + N_L = N$). The set of possible photon imbalances I has a probability distribution, $\mathcal{P}(I)$. The imbalance distribution depends on the lattice constant and the degree of intrinsic (single-qubit) chirality of the waveguide.

In the mirror configuration, as the left and right operators are identical, the normalized probability of emitting a photon in each direction reduces to approximately $p_{L/R}$ at any stage of the decay. Hence, the photon imbalance roughly follows the binomial distribution

$$\mathcal{P}(I) \simeq \frac{N!}{\left(\frac{N+I}{2}\right)! \left(\frac{N-I}{2}\right)!} \left(\frac{\Gamma_L}{\Gamma_{1D}}\right)^{\frac{N-I}{2}} \left(\frac{\Gamma_R}{\Gamma_{1D}}\right)^{\frac{N+I}{2}}. \quad (15)$$

As shown in Fig. 3(b), this analytical expression is in good agreement with the results obtained by the numerical evolution using quantum trajectories. Minor discrepancies originate from the action of the Hamiltonian in between jumps (only for a chiral waveguide) and noise from the finite number of trajectories.

Outside the mirror configuration, the repeated action of a jump operator enhances its probability of acting again, thus amplifying the initial fluctuation and either breaking mirror symmetry (for a bidirectional waveguide) or collectively enhancing chirality (for a chiral one). This process mostly occurs in trajectories that finish at early times (for which time between jumps is small and Hamiltonian evolution is negligible). This is shown in Fig. 3(c). For a bidirectional waveguide, almost all of the photons are emitted in one direction. A mildly-chiral waveguide becomes almost perfectly chiral.

On average, photons are not radiated as fast as in Dicke's scenario, so the Hamiltonian evolution becomes relevant for the imbalance statistics at later times. Hamiltonian evolution scrambles the states (and thus final jumps lose their enhancement), as shown in Fig. 3(d). For the bidirectional waveguide, it gives rise to an almost-flat imbalance distribution. For the chiral waveguide, the enhancement of the chirality is reduced. Nonetheless, the probability of detecting all photons in a single direction is much greater than the probability predicted by the binomial distribution for independent emission. This resembles a recent prediction for multilevel atoms in a cavity, where there is a higher probability of large imbalances between ground state populations compared to predictions from a single atom [41].

In conclusion, we found the minimal conditions for an ensemble of qubits to emit a superradiant burst into a 1D bath. We estimate that a superradiant burst is observable in different experimental setups such as superconducting qubits coupled to transmission lines and atoms coupled to nanofibers. Many-body superradiance gives rise to an emergent chirality in the system, with large amounts of photons being emitted in one direction. The photon state produced in the mirror configuration is known to have a large overlap with a multi-photon Fock state, and shares similar metrological properties [42–46]. However, photons need to be recombined into a single pulse, as they are emitted in both directions. This issue is partially overcome at different lattice constants or in chiral waveguides. However, in these cases, the Hamiltonian dynamics may populate dark states, which are prevalent at low excitation densities [7, 47], trapping the last few photons in the pulse. We will investigate the quantum state of the photons produced via many-body decay in subsequent work. Another promising line of inquiry involves the possibility of accessing entangled dark states by combining dissipative evolution with measurement and feedback control.

Acknowledgments – We are thankful to J. T. Lee,

R. Gutiérrez-Jáuregui, W. Pfaff, W.-K. Mok, and L.-C. Kwek for stimulating discussions. We gratefully acknowledge support from the Air Force Office of Scientific Research through their Young Investigator Prize (grant No. 21RT0751), the National Science Foundation through their CAREER Award (No. 2047380), the A. P. Sloan foundation, and the David and Lucile Packard foundation. S. C.-L. acknowledges additional support from the Chien-Shiung Wu Family Foundation. A.A.-G. also acknowledges the Flatiron Institute, where some of this work was performed. We acknowledge computing resources from Columbia University's Shared Research Computing Facility project, which is supported by NIH Research Facility Improvement Grant 1G20RR030893-01, and associated funds from the New York State Empire State Development, Division of Science Technology and Innovation (NYSTAR) Contract C090171, both awarded April 15, 2010.

* ana.asenjo@columbia.edu

- [1] E. M. Purcell, Spontaneous emission probabilities at radio frequencies, *Phys. Rev.* **69**, 674 (1946).
- [2] D. Kleppner, Inhibited spontaneous emission, *Phys. Rev. Lett.* **47**, 233 (1981).
- [3] S. Haroche and D. Kleppner, Cavity quantum electrodynamics, *Physics Today* **42**, 24 (1989).
- [4] E. Vetsch, D. Reitz, G. Sagué, R. Schmidt, S. T. Dawkins, and A. Rauschenbeutel, Optical interface created by laser-cooled atoms trapped in the evanescent field surrounding an optical nanofiber, *Phys. Rev. Lett.* **104**, 203603 (2010).
- [5] A. Goban, K. S. Choi, D. J. Alton, D. Ding, C. Lacroûte, M. Pototschnig, T. Thiele, N. P. Stern, and H. J. Kimble, Demonstration of a state-insensitive, compensated nanofiber trap, *Phys. Rev. Lett.* **109**, 033603 (2012).
- [6] B. Gouraud, D. Maxein, A. Nicolas, O. Morin, and J. Laurat, Demonstration of a memory for tightly guided light in an optical nanofiber, *Phys. Rev. Lett.* **114**, 180503 (2015).
- [7] P. Solano, P. Barberis-Blostein, F. K. Fatemi, L. A. Orozco, and S. L. Rolston, Super-radiance reveals infinite-range dipole interactions through a nanofiber, *Nat. Commun.* **8**, 1857 (2017).
- [8] J. D. Thompson, T. G. Tiecke, N. P. de Leon, J. Feist, A. V. Akimov, M. Gullans, A. S. Zibrov, V. Vuletić, and M. D. Lukin, Coupling a single trapped atom to a nanoscale optical cavity, *Science* **340**, 1202 (2013).
- [9] A. Goban, C.-L. Hung, J. D. Hood, S.-P. Yu, J. A. Muniz, O. Painter, and H. J. Kimble, Superradiance for atoms trapped along a photonic crystal waveguide, *Phys. Rev. Lett.* **115**, 063601 (2015).
- [10] J. D. Hood, A. Goban, A. Asenjo-Garcia, M. Lu, S.-P. Yu, D. E. Chang, and H. J. Kimble, Atom-atom interactions around the band edge of a photonic crystal waveguide, *Proc. Natl. Acad. Sci. USA* **113**, 10507 (2016).
- [11] Y. Liu and A. A. Houck, Quantum electrodynamics near a photonic bandgap, *Nat. Phys.* **13**, 48 (2016).
- [12] M. Mirhosseini, E. Kim, X. Zhang, A. Sipahigil, P. B.

- Dieterle, A. J. Keller, A. Asenjo-Garcia, D. E. Chang, and O. Painter, Cavity quantum electrodynamics with atom-like mirrors, *Nature* **569**, 692 (2019).
- [13] M. Zanner, T. Orell, C. M. F. Schneider, R. Albert, S. Oleschko, M. L. Juan, M. Silveri, and G. Kirchmair, Coherent control of a multi-qubit dark state in waveguide quantum electrodynamics, *Nature Physics* **18**, 538 (2022).
- [14] T. Ramos, H. Pichler, A. J. Daley, and P. Zoller, Quantum spin dimers from chiral dissipation in cold-atom chains, *Phys. Rev. Lett.* **113**, 237203 (2014).
- [15] N. Fayard, L. Henriët, A. Asenjo-Garcia, and D. E. Chang, Many-body localization in waveguide quantum electrodynamics, *Phys. Rev. Research* **3**, 033233 (2021).
- [16] A. Albrecht, L. Henriët, A. Asenjo-Garcia, P. B. Dieterle, O. Painter, and D. E. Chang, Subradiant states of quantum bits coupled to a one-dimensional waveguide, *New Journal of Physics* **21**, 025003 (2019).
- [17] R. H. Dicke, Coherence in spontaneous radiation processes, *Phys. Rev.* **93**, 99 (1954).
- [18] M. Gross and S. Haroche, Superradiance: An essay on the theory of collective spontaneous emission, *Physics Reports* **93**, 301 (1982).
- [19] N. E. Rehler and J. H. Eberly, Superradiance, *Phys. Rev. A* **3**, 1735 (1971).
- [20] R. Friedberg, S. Hartmann, and J. Manassah, Limited superradiant damping of small samples, *Physics Letters A* **40**, 365 (1972).
- [21] N. Skribanowitz, I. P. Herman, J. C. MacGillivray, and M. S. Feld, Observation of Dicke superradiance in optically pumped HF gas, *Phys. Rev. Lett.* **30**, 309 (1973).
- [22] A. Flusberg, T. Mossberg, and S. Hartmann, Observation of Dicke superradiance at $1.30\ \mu\text{m}$ in atomic Tl vapor, *Physics Letters A* **58**, 373 (1976).
- [23] M. Gross, C. Fabre, P. Pillet, and S. Haroche, Observation of near-infrared Dicke superradiance on cascading transitions in atomic sodium, *Phys. Rev. Lett.* **36**, 1035 (1976).
- [24] J. P. Clemens, L. Horvath, B. C. Sanders, and H. J. Carmichael, Collective spontaneous emission from a line of atoms, *Phys. Rev. A* **68**, 023809 (2003).
- [25] S. J. Masson, I. Ferrier-Barbut, L. A. Orozco, A. Browaeys, and A. Asenjo-Garcia, Many-body signatures of collective decay in atomic chains, *Phys. Rev. Lett.* **125**, 263601 (2020).
- [26] O. Rubies-Bigorda and S. F. Yelin, Superradiance and subradiance in inverted atomic arrays (2021), arXiv:2110.11288.
- [27] F. Robicheaux, Theoretical study of early-time superradiance for atom clouds and arrays, *Phys. Rev. A* **104**, 063706 (2021).
- [28] G. Ferioli, A. Glicenstein, F. Robicheaux, R. T. Sutherland, A. Browaeys, and I. Ferrier-Barbut, Laser-driven superradiant ensembles of two-level atoms near Dicke regime, *Phys. Rev. Lett.* **127**, 243602 (2021).
- [29] S. J. Masson and A. Asenjo-Garcia, Universality of Dicke superradiance in arrays of quantum emitters, *Nature Communications* **13**, 2285 (2022).
- [30] E. Sierra, S. J. Masson, and A. Asenjo-Garcia, Dicke superradiance in ordered lattices: Dimensionality matters, *Phys. Rev. Research* **4**, 023207 (2022).
- [31] T. Orell, M. Zanner, M. L. Juan, A. Sharafiev, R. Albert, S. Oleschko, G. Kirchmair, and M. Silveri, Collective bosonic effects in an array of transmon devices, *Phys. Rev. A* **105**, 063701 (2022).
- [32] T. Gruner and D.-G. Welsch, Green-function approach to the radiation-field quantization for homogeneous and inhomogeneous Kramers-Kronig dielectrics, *Phys. Rev. A* **53**, 1818 (1996).
- [33] H. T. Dung, L. Knöll, and D.-G. Welsch, Resonant dipole-dipole interaction in the presence of dispersing and absorbing surroundings, *Phys. Rev. A* **66**, 063810 (2002).
- [34] H. Pichler, T. Ramos, A. J. Daley, and P. Zoller, Quantum optics of chiral spin networks, *Phys. Rev. A* **91**, 042116 (2015).
- [35] H. Carmichael and K. Kim, A quantum trajectory unraveling of the superradiance master equation, *Opt. Commun.* **179**, 417 (2000).
- [36] J. Dalibard, Y. Castin, and K. Mølmer, Wave-function approach to dissipative processes in quantum optics, *Phys. Rev. Lett.* **68**, 580 (1992).
- [37] H. Carmichael, *An open systems approach to Quantum Optics* (Springer-Verlag, Berlin, Heidelberg, 1993).
- [38] D. E. Chang, L. Jiang, A. V. Gorshkov, and H. J. Kimble, Cavity QED with atomic mirrors, *New Journal of Physics* **14**, 063003 (2012).
- [39] N. V. Corzo, B. Gouraud, A. Chandra, A. Goban, A. S. Sheremet, D. V. Kupriyanov, and J. Laurat, Large Bragg reflection from one-dimensional chains of trapped atoms near a nanoscale waveguide, *Phys. Rev. Lett.* **117**, 133603 (2016).
- [40] H. L. Sørensen, J.-B. Béguin, K. W. Kluge, I. Iakoupov, A. S. Sørensen, J. H. Müller, E. S. Polzik, and J. Appel, Coherent backscattering of light off one-dimensional atomic strings, *Phys. Rev. Lett.* **117**, 133604 (2016).
- [41] A. Piñeiro Orioli, J. K. Thompson, and A. M. Rey, Emergent dark states from superradiant dynamics in multi-level atoms in a cavity, *Phys. Rev. X* **12**, 011054 (2022).
- [42] A. González-Tudela, V. Paulisch, D. E. Chang, H. J. Kimble, and J. I. Cirac, Deterministic generation of arbitrary photonic states assisted by dissipation, *Phys. Rev. Lett.* **115**, 163603 (2015).
- [43] V. Paulisch, M. Perarnau-Llobet, A. González-Tudela, and J. I. Cirac, Quantum metrology with one-dimensional superradiant photonic states, *Phys. Rev. A* **99**, 043807 (2019).
- [44] C. Groiseau, A. E. J. Elliott, S. J. Masson, and S. Parkins, Proposal for a deterministic single-atom source of quasisuperradiant N-photon pulses, *Phys. Rev. Lett.* **127**, 033602 (2021).
- [45] M. Perarnau-Llobet, A. González-Tudela, and J. I. Cirac, Multimode Fock states with large photon number: effective descriptions and applications in quantum metrology, *Quantum Science and Technology* **5**, 025003 (2020).
- [46] B. Lemberger and K. Mølmer, Radiation eigenmodes of Dicke superradiance, *Phys. Rev. A* **103**, 033713 (2021).
- [47] G. Ferioli, A. Glicenstein, L. Henriët, I. Ferrier-Barbut, and A. Browaeys, Storage and release of subradiant excitations in a dense atomic cloud, *Phys. Rev. X* **11**, 021031 (2021).

SUPPLEMENTAL INFORMATION

1. Calculation of the conditional statistics

A necessary condition for observing a burst in a detector placed at the end of the waveguide is that the emission of photons into the waveguide increases at $t = 0$. This condition can be written as $\tilde{g}^{(2)}(0) > 1$, where the second-order correlation function reads

$$\tilde{g}^{(2)}(0) = \frac{\sum_{\nu=+,-} \sum_{\mu=+,-,i} \Gamma_\nu \Gamma_\mu \langle \hat{\sigma}_\mu^\dagger \hat{\sigma}_\nu^\dagger \hat{\sigma}_\nu \hat{\sigma}_\mu \rangle}{\left(\sum_{\nu=+,-} \Gamma_\nu \langle \hat{\sigma}_\nu^\dagger \hat{\sigma}_\nu \rangle \right) \left(\sum_{\mu=+,-,i} \Gamma_\mu \langle \hat{\sigma}_\mu^\dagger \hat{\sigma}_\mu \rangle \right)} = 1 + \frac{\sum_{\nu=+,-} \Gamma_\nu^2 - N\Gamma_{1D}(2\Gamma_{1D} + \Gamma')}{N^2\Gamma_{1D}(\Gamma_{1D} + \Gamma')}. \quad (16)$$

The condition $\tilde{g}^{(2)}(0) > 1$ implies $\text{Tr}[\mathbb{F}^2] > N\Gamma_{1D}(2\Gamma_{1D} + \Gamma')$. The variance of $\{\Gamma_\nu\}$,

$$\text{Var}\left(\frac{\{\Gamma_\nu\}}{\Gamma_{1D}}\right) = \frac{1}{N\Gamma_{1D}^2} \sum_{\nu=+,-} (\Gamma_\nu^2 - \Gamma_{1D}^2), \quad (17)$$

can be used to rewrite this expression as Eq. (7) of the main text.

1.1. Minimal burst condition for arbitrary spatial configurations

Even when the analytical expression of the eigenvalues is not known, one can obtain a condition that guarantees a burst by finding a lower bound for $\sum_\nu \Gamma_\nu^2 \equiv \text{Tr}[\mathbb{F}^2]$. The trace of \mathbb{F}^2 for an arbitrary spatial configuration is readily calculated as

$$\begin{aligned} \text{Tr}[\mathbb{F}^2] &= \sum_{i,j=1}^N \Gamma_{ij}^g \Gamma_{ji}^g = N^2(\Gamma_R^2 + \Gamma_L^2) + 2\Gamma_R\Gamma_L \sum_{i,j=1}^N \cos(2k_{1D}(z_i - z_j)) \\ &= N^2(\Gamma_R^2 + \Gamma_L^2) + 2\Gamma_R\Gamma_L \left[\left(\sum_{i=1}^N \cos(2k_{1D}z_i) \right)^2 + \left(\sum_{i=1}^N \sin(2k_{1D}z_i) \right)^2 \right] \geq N^2(\Gamma_R^2 + \Gamma_L^2). \end{aligned} \quad (18)$$

Thus, choosing a set of parameters that satisfies $N(\Gamma_R^2 + \Gamma_L^2) > \Gamma_{1D}(2\Gamma_{1D} + \Gamma')$, i.e., Eq. (10) in the main text, guarantees superradiance regardless of the arrangement of the qubits. If the qubits form an ordered array with lattice constant $k_{1D}d = n\pi/N$ [i.e. at the degeneracy points in Fig. 2(a)], the bound is saturated. This can be intuitively understood from the fact that $\text{Tr}[\mathbb{F}^2]$ is related to the variance of $\{\Gamma_\nu\}$, which is minimized at degeneracy.

1.2. Enhancement of the emission of the third photon

To confirm that $\tilde{g}^{(2)}(0) > 1$ is a sufficient condition to predict a burst, we compute the conditional third order correlation function, which reads

$$\begin{aligned} \tilde{g}^{(3)}(0) &= \frac{\sum_{\nu=+,-} \sum_{\mu,\chi=+,-,i} \Gamma_\nu \Gamma_\mu \Gamma_\chi \langle \hat{\sigma}_\chi^\dagger \hat{\sigma}_\mu^\dagger \hat{\sigma}_\nu^\dagger \hat{\sigma}_\nu \hat{\sigma}_\mu \hat{\sigma}_\chi \rangle}{\left(\sum_{\nu=+,-} \Gamma_\nu \langle \hat{\sigma}_\nu^\dagger \hat{\sigma}_\nu \rangle \right) \left(\sum_{\mu=+,-,i} \Gamma_\mu \langle \hat{\sigma}_\mu^\dagger \hat{\sigma}_\mu \rangle \right)^2} \\ &= 1 - \frac{6\Gamma_{1D}^2 + 8\Gamma'\Gamma_{1D} + 3\Gamma'^2}{N(\Gamma_{1D} + \Gamma')^2} + \frac{12\Gamma_{1D}^2 + 8\Gamma'\Gamma_{1D} + 2\Gamma'^2}{N^2(\Gamma_{1D} + \Gamma')^2} \\ &\quad + \frac{(3N\Gamma_{1D} - 12\Gamma_{1D} + 2(N-2)\Gamma') \sum_{\nu=+,-} \Gamma_\nu^2 + 2 \sum_{\nu=+,-} \Gamma_\nu^3}{N^3\Gamma_{1D}(\Gamma_{1D} + \Gamma')^2}. \end{aligned} \quad (19)$$

$$\quad (20)$$

Below we prove by contradiction that there is no combination of parameters such that $\tilde{g}^{(2)}(0) \leq 1$ while $\tilde{g}^{(3)}(0) > 1$, so the emission of the third photon is never enhanced if the second was not. The inequality $\tilde{g}^{(2)}(0) \leq 1$ implies

$$\text{Tr}[\mathbb{F}^2] < N\Gamma_{1D}(2\Gamma_{1D} + \Gamma'). \quad (21)$$

Combining the above equation with $\tilde{g}^{(3)}(0) > 1$ yields

$$2\text{Tr}[\mathbb{F}^3] > N^2\Gamma_{1D}\Gamma'(\Gamma_{1D} + \Gamma') + 2N\Gamma_{1D}(6\Gamma_{1D}^2 + 6\Gamma_{1D}\Gamma' + \Gamma'^2). \quad (22)$$

After some algebraic manipulations, one finds

$$\text{Tr}[\mathbb{F}^2] = \sum_{i,j=1}^N \Gamma_{ij}\Gamma_{ji} = N^2(\Gamma_L^2 + \Gamma_R^2) + 2\Gamma_L\Gamma_R \sum_{i,j=1}^N \cos[2k_{1D}(z_i - z_j)], \quad (23a)$$

$$\text{Tr}[\mathbb{F}^3] = \sum_{i,j,k=1}^N \Gamma_{ij}\Gamma_{jk}\Gamma_{ki} = N^3(\Gamma_L^3 + \Gamma_R^3) + 3N\Gamma_{1D}\Gamma_L\Gamma_R \sum_{i,j=1}^N \cos[2k_{1D}(z_i - z_j)]. \quad (23b)$$

Therefore, the condition for the third emission to be the first one that is enhanced reduces to

$$F(N) \equiv N^2 + BN + C < 0, \quad (24)$$

with

$$B = \left(\frac{\Gamma'}{\Gamma_{1D}}\right)^2 - \frac{2\Gamma'}{\Gamma_{1D}} - 6, \quad (25a)$$

$$C = 2\left(\frac{\Gamma'}{\Gamma_{1D}}\right)^2 + 12 + 12\frac{\Gamma'}{\Gamma_{1D}}. \quad (25b)$$

While $C > 0$ for all possible values of the ratio Γ_{1D}/Γ' , $B > 0$ only if $\Gamma'/\Gamma_{1D} > 1 + \sqrt{7}$. Thus, if $\Gamma'/\Gamma_{1D} > 1 + \sqrt{7}$, the inequality in Eq. (24) is never satisfied. If $\Gamma'/\Gamma_{1D} < 1 + \sqrt{7}$, the discriminant of $F(N)$ is negative, so $F(N)$ does not have real roots and hence it is never negative. We then conclude that no combination of parameters yield $\tilde{g}^{(2)}(0) \leq 1$ while $\tilde{g}^{(3)}(0) > 1$, so $\tilde{g}^{(2)}(0) > 1$ is a sufficient condition to predict a burst.

2. Emergent translational symmetry at the degeneracy points

Consider a finite and ordered array of N qubits whose interactions are described through the matrix of coefficients Γ_{ij} . If the interactions satisfy periodic or antiperiodic boundary conditions (i.e. if $\Gamma_{i,N+1} = \pm\Gamma_{i,1}$), the system becomes translationally invariant since one can identify particle 1 with particle $N + 1$. Periodic boundary conditions (PBC) emerge for bidirectional waveguides at lattice constants $k_{1D}d = 2n\pi/N$, with $n \in \mathbb{N}$. Antiperiodic boundary conditions (APBC) are achieved for $k_{1D}d = (2n+1)\pi/N$. Therefore, at $k_{1D}d = n\pi/N$, the eigenvectors of \mathbb{F} must obey Bloch's theorem. The jump operators thus take the form of annihilation operators for spin waves with momentum k in the first Brillouin zone, i.e.,

$$\hat{S}_k = \frac{1}{\sqrt{N}} \sum_{j=1}^N e^{-ikdj} \hat{\sigma}_{ge}^j. \quad (26)$$

The only two jump operators with finite decay rates are those that match the wavevector of the guided mode, i.e., $k = \pm k_{1D}$. These are the left and right jump operators defined in Eq. (11) of the main text. Since the system is mirror-symmetric, the two jump operators must have identical decay rates. Thus, the two non-zero eigenvalues of the \mathbb{F} matrix become degenerate at $k_{1D}d = n\pi/N$.

We can also demonstrate that the two non-zero eigenvalues are degenerate at $k_{1D}d = n\pi/N$ by employing the analytical form of the collective jump operators. For the case of a bidirectional waveguide they read

$$\hat{\mathcal{O}}_{\pm} = \sqrt{\frac{\Gamma_{1D}}{\Gamma_{\pm}}} \sum_{i=1}^N \mathcal{F}_{\pm} \left[k_{1D}d \left(\frac{N+1}{2} - i \right) \right] \hat{\sigma}_{ge}^i, \quad (27)$$

with $\mathcal{F}_{\{+(-)\}}[\cdot] = \cos[\cdot](\sin[\cdot])$. Notice that $\hat{\mathcal{O}}_{\pm}$ differ by a $\pi/2$ phase shift. Due to the emergent translational symmetry at $k_{1D}d = n\pi/N$, $\hat{\mathcal{O}}_{\pm}$ must have the same decay rates at these points.

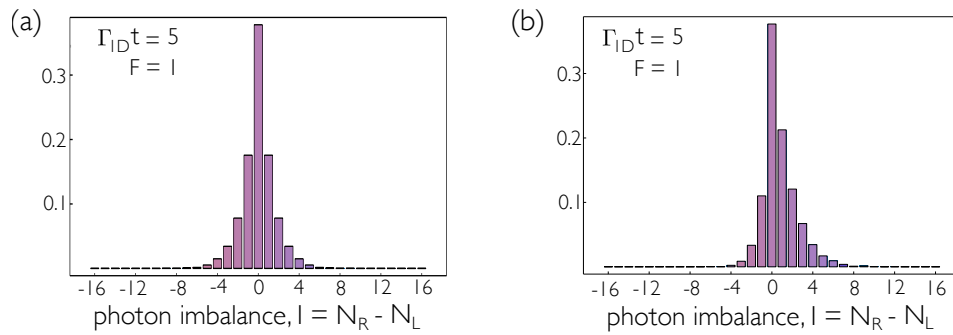


FIG. 4. Imbalance statistics on the emission direction for 16 qubits with large parasitic decay ($\Gamma' = 10\Gamma_{1D}$) emitting into a (a) bidirectional and (b) a chiral waveguide ($\Gamma_R = 3\Gamma_L$).

3. Imbalance statistics with large parasitic decay and details on numerical evolution

If the parasitic decay dominates, correlations are washed out, and the imbalance distribution is centered around zero, displaying very suppressed probabilities of large imbalances, as shown in Fig. 4. The possible values for I are now $\{-N, -N + 1, \dots, N\}$ since N_L and N_R can take any value as long as $N_R + N_L \leq N$.

The number of trajectories used for Figs. 1 and 3 (on the main text), and SI Fig. 1 is detailed in Table I.

TABLE I. Number of trajectories used for Figs. 1 and 3 of the main text, and SI Fig. 1

	Bidirectional	Chiral
Fig. 1	2,000	2,000
Fig. 3(b)	12,000	12,000
Fig. 3(c) and Fig. 3(d)	20,000	13,000
SI Fig. 1	5,000	8,000

The calculations for Figs. 2(b) and 2(c) are performed in the constrained Hilbert space composed of states with at most two atoms in $|g\rangle$. A burst is predicted if the emission rate at the final time $N\Gamma_{1D}t_{\text{fin}} = 10^{-5}$ is larger than at $t = 0$. The probability in Fig. 2(c) is computed with 100 random configurations. The numerical boundary is defined such that the burst prediction occurs in every configuration.